**RAMAN IMAGING OF EXTRATERRESTRIAL MATERIALS.** Hongwei Du and Alian Wang, Dept. of Earth & Planetary Sciences, McDonnell Center for the Space Sciences, Washington University in St. Louis (h.du@levee.wustl.edu, alianw@levee.wustl.edu )

**Raman imaging:** A Raman imaging system provides *molecular maps*, similar to the *element map* provided by an electron microprobe or scanning electron microscope. It collects a spectral image cube from a sample, then generates a map of minerals, molecular species ($H_2O$/OH) and chemical bonds (e.g., C-H, N-H, C-O, etc). These images can show spatial distribution, abundance, chemical zoning, and shock induced mechanical stress of a phase, based on its Raman peak position, peak intensity, peak shift, and peak width. The spatial correlations of various phases reveal evidence of past physical, chemical, and biological processes, as well as *genetic relationships* of the different phases [1].

Various methodologies exist to accomplish Raman imaging. AOTF (Acoustic Optical Tunable Filter) technology was used in the early 2000s, but was not particularly successful for geological samples. Methodologies that have been developed recently include: (1) using a high accuracy moving microscopic stage to position sequentially the spots from a selected area of a sample under the laser beam; (2) using a galvonometric motor to scan the laser beam onto the spots of a small area of a sample, then to combine the X-Y motion of a microscopic stage to enlarge the imaged area; (3) using a defocused laser beam with an elongated spot, then combining a one-D motion of a microscopic stage to make 2D image and to reduce the time duration of the measurement; (4) a combination of laser optics, high accuracy stage motion and CCD readout electronics for fast Raman imaging of large area.

**A Raman imager with multiple laser lines:** In the fall of 2011, we built a new Raman imaging laboratory and installed an inVia® Raman System (Renishaw Company). The system consists of a spectrometer capable of collecting Raman spectra excited by five excitation laser lines. It is also an imager that can use methodologies (1), (3), and (4) described above to make high quality Raman images. It uses a high accuracy microscopic stage with a step size of 100 nm, which, in combination with a laser beam diameter at diffraction limit (< 1 μm), can generate a Raman image with spatial resolution of ~ 250-300 nm in the X-Y plane and ~ 500 nm in the Z direction. When using methodology (4), the Raman image from a large area can be obtained in less than 10 minutes (Streamline™ mode). In addition, the system has a function for making direct global Raman imaging using angle-adjusting-filters (instead of AOTF).

No special need for surface preparation of the analyzed sample. Soild samples such as thin section, sawn slice of rock chip, mineral powder or soils, liquid samples in capillary, glass bottle or petri dish can all be analyzed.

Laser Raman spectroscopy (LRS) observes the spectral shifts (Raman shift $\Delta\lambda$) from an excitation wavelength ($\lambda_0$) caused by the molecular vibrations of chemical bonds in a sample. Thus LRS can work in IR, VIS, UV, and even X-ray spectral ranges. A Raman system with multiple excitation laser wavelengths is able to study a wide variety of materials. Raman cross sections of materials change with excitation wavelengths. Some laser wavelengths enhance Raman signals by inducing Raman resonance effects. Some laser wavelengths help to avoid the interference of fluorescence generated by specific species in the samples. Our new Raman imaging system has five laser wavelengths: 785 nm line of a diode laser, 632.8 nm line of a He-Ne laser, 532nm line of a diode pumped solid state laser, 442 nm line and 325 nm line of a He-Cd laser.

Up to now, the green laser excitation (e.g., 532 nm) has been demonstrated to be the most efficient one for the characterization of general mineralogy and biomarker such as carotenoids [2, 3], whereas UV (<400 nm) and IR (785 nm) laser excitations have been suggested to have advantages for the detection of DNA, RNA, and proteins [4, 5]. The new laboratory Raman imaging system with multiple excitation wavelengths provides the flexibility to study unknown samples, especially those returned from planetary missions in the past and in the future.

**Raman imaging of extraterrestrial materials:** Five types of extraterrestrial materials were selected for a preliminary Raman imaging investigation: Apollo lunar sample, lunar meteorites, Martian meteorites, achondrites, and carbonaceous chondrites.

Figure 1 shows Raman spectra and Raman images that we obtained from Apollo sample 14161-7062, a thin section of a KREEP-rich impact-melt rock [6]. Two areas were studied. Area A is a mesostasis region adjacent to plagioclase and clino-pyroxene grains (A1). Six sets of imaging measurements were taken, using a 532 nm laser line. In a specific mesostasis region (A4 & A5), baddeleyite [$ZrO_2$] was found co-existing with ilmenite [$FeTiO_3$] along with RE-merrillite [$REE_2Ca_{16}(Mg,Fe^{2+})_2(PO_4)_{14}$]. The strong peaks in 400-1000 $cm^{-1}$ spectral range are actually REE fluorescent peaks caused by the high REE contents in baddeleyite. As shown in A3 spectral panel, the Raman spec-

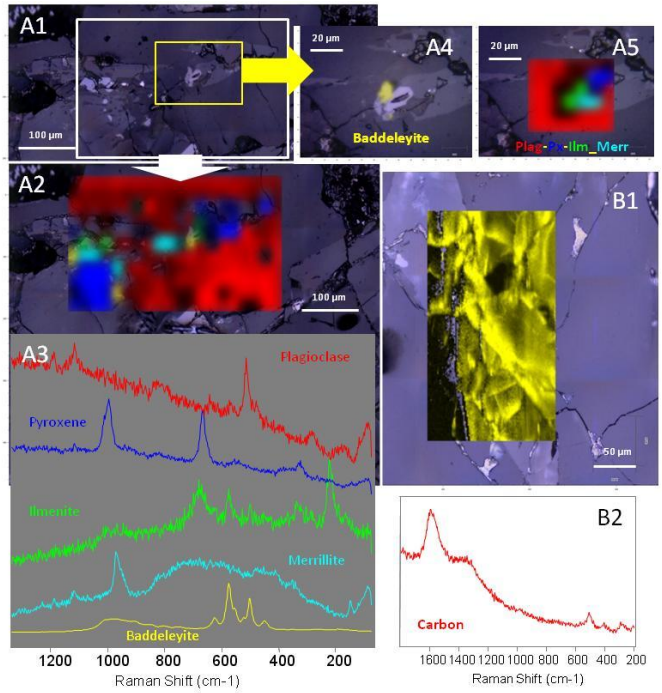


Figure 1. Raman spectra and Raman images of Apollo 14161-7062 (thin section). A1-A5: a mesostasis area; B1-B2: remained carbon in fractures after the removal of C-coat prior Raman analysis.

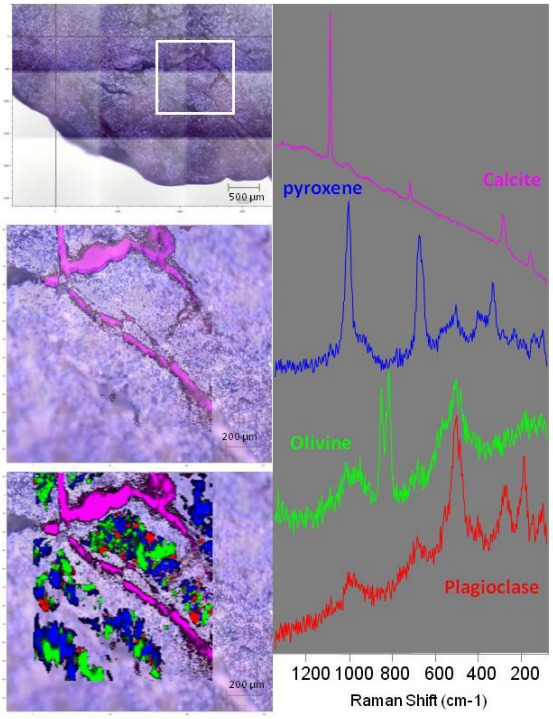


Figure 2. Raman images of a sawn slice of lunar meteorite Dhofar 1627 showing the three main lunar minerals and terrestrial calcite filling fractures.

tra from ordinary lunar minerals are much weaker than baddeleyite, which creates a challenge for making the phase distribution map in this region. From a Raman imaging scan of a larger area (A2), baddeleyite, ilmenite and RE-merrillite were found again near a pyroxene grain (low-left corner of A2).

B1 in Figure 1 shows the abundance map of carbon in a matrix area B of the same thin section (using 442 nm laser line). These amorphous carbon molecules (Raman spectrum in B2) entered the fractures in mineral grains during the C-coating process for EMP analysis, and remained there after removal the surface C-coat by polishing prior to Raman analysis.

Figure 2 shows the Raman spectra and Raman images that we obtained from a sawn face of lunar meteorite Dhofar 1672 [7]. Terrestrial calcite fills the fractures in this rock. The dark spots in A2 of Figure 1 or unfilled space in the lowest image of Figure 2 have either low spectral S/N or multiphases spectrum with generally low S/N for each phase. We chose to not fill these spots for the purpose of making less "busy" images.

**Acknowledgement:** The purchase of new Raman system was fund by NASA Major Planetary Equipment program under Mars Fundamental Research project NNX10AM89G, and by McDonnell Center for the Space Sciences, Dept of Earth and Planetary Sciences, and School of Arts and Sciences at Washington University in St. Louis. We would also thank for the supports from NASA for an ASTEP project NNX09AE80A subcontract #08-SC-1072 and for a MoO project (RLS_ExoMars) contract #1295053, both are related to Planetary Raman Spectroscopy. We thank our colleagues of Planetary Material Research Group at WUSTL-EPSC, Randy Korotev and Bradley Jolliff, for providing lunar samples for this preliminary study.

**References:** [1] Steele et al. (2007) *Meteorite Planet. Sci.*, 42:1549–1566. [2] Marshall & Wang (2010), *9th GeoRaman conference*. [3] Marshall et al. (2010) *Astrobiology*, 10, DOI: 10.1089/ast.2009.0344. [4] Edwards et al. (2005) *Icarus*, 174, p560. [5] Villar et al (2005) *Orig. Life Evol.Biosph*, 35, p489. [6] Haskin et al. (1997) *JGR*, 102 p19293. [7] Korotev et al., *this conf.*